Supported by

Neutral Transport Simulations of Gas Puff Imaging Experiments on NSTX

D. P. Stotler, D. A. D'Ippolito[1], B. LeBlanc, R. J. Maqueda[2], J. R. Myra[1], S. A. Sabbagh[3], and S. J. Zweben

Princeton Plasma Physics Laboratory
Princeton University, Princeton NJ 08543

[1]Lodestar Research Corporation, Boulder CO 80301
[2]Los Alamos National Laboratory, Los Alamos NM 87545
[3]Columbia University, New York NY 10027

Columbia U
Comp-X
General Atomics
INEL
Johns Hopkins U
LANL
LLNL
Lodestar
MIT
Nova Photonics
NYU
ORNL
PPPL
PSI
SNL
UC Davis
UC Irvine
UCLA
UCSD
U Maryland
U New Mexico
U Rochester
U Washington
U Wisconsin
Culham Sci Ctr
Hiroshima U
HIST
Kyushu Tokai U
Niigata U
Tsukuba U
U Tokyo
JAERI
Ioffe Inst
TRINITI
KBSI
KAIST
ENEA, Frascati
CEA, Cadarache
IPP, Jülich
IPP, Garching
U Quebec

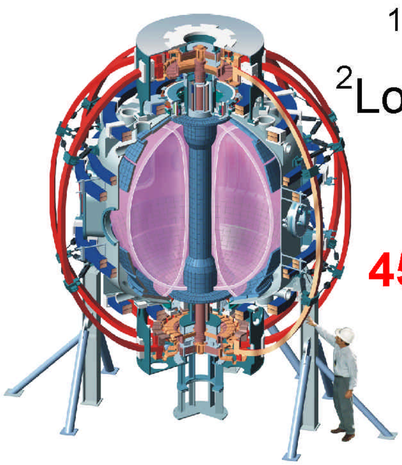

45th Annual Meeting of Division of Plasma Physics
American Physical Society
October 27 – 31, 2003
Albuquerque, New Mexico

Gas Puff Imaging (GPI) Experiments Designed to Measure 2-D Structure of Edge Turbulence

- Puff neutral gas near outer wall,
- View with fast camera fluctuating visible emission resulting from electron impact excitation of that gas,
  - Compare with 3-D nonlinear plasma simulation codes,
  - Reduced theoretical turbulence models,
  - And with turbulence measured by probes.
- NSTX GPI geometry optimizes data quality,
  - But, 3-D arrangement complicates interpretation,
  - $\Rightarrow$ extend DEGAS 2 Monte Carlo neutral transport simulations to 3-D.

OUTLINE

1. Describe GPI experiments,
2. Construction of 3-D DEGAS 2 Simulations,
3. Benchmark code against experiment,
4. Estimate diagnostic resolution,
5. Use neutral density to infer 2-D plasma profiles from GPI images.

1. Description of GPI Experiments

See also poster LP1.006,

“2-D Imaging of Edge Turbulence in NSTX and Alcator C-Mod”, Lowrance et al.

Gas Puff Imaging Hardware Configuration in NSTX

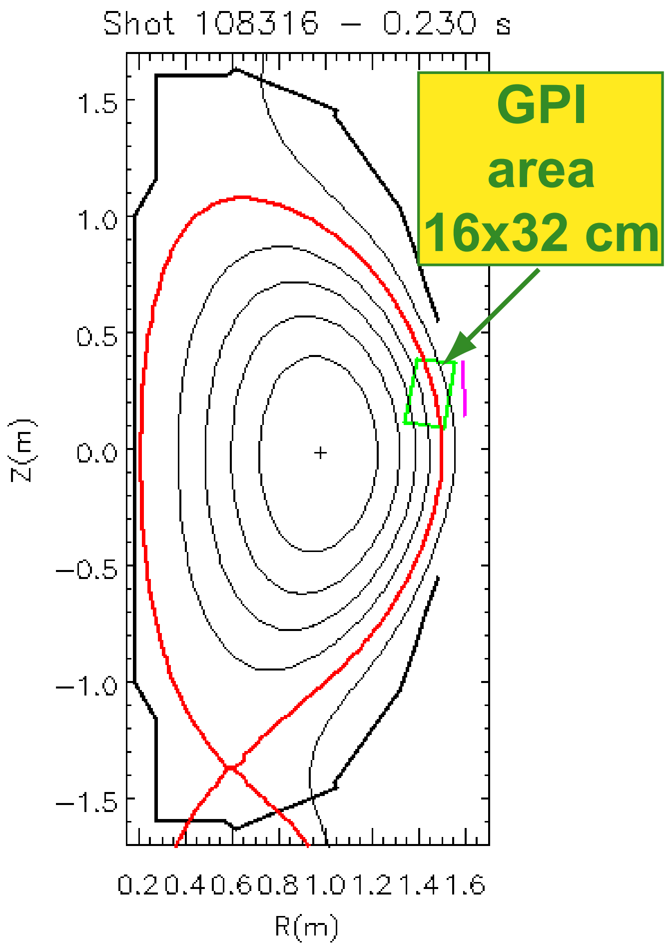

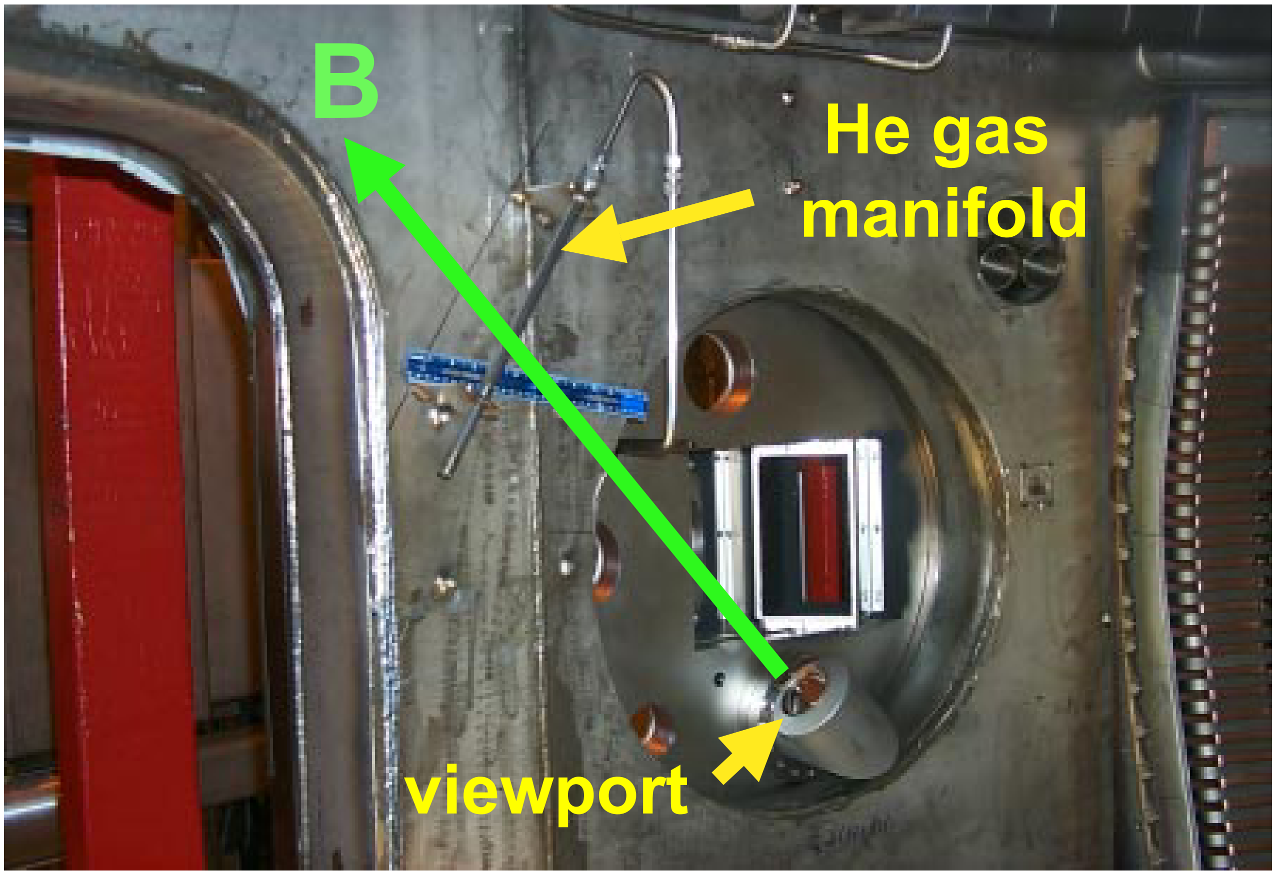

Camera Records Fluctuating 587.6 nm He I Emission for 28 Frames @10µs/frame

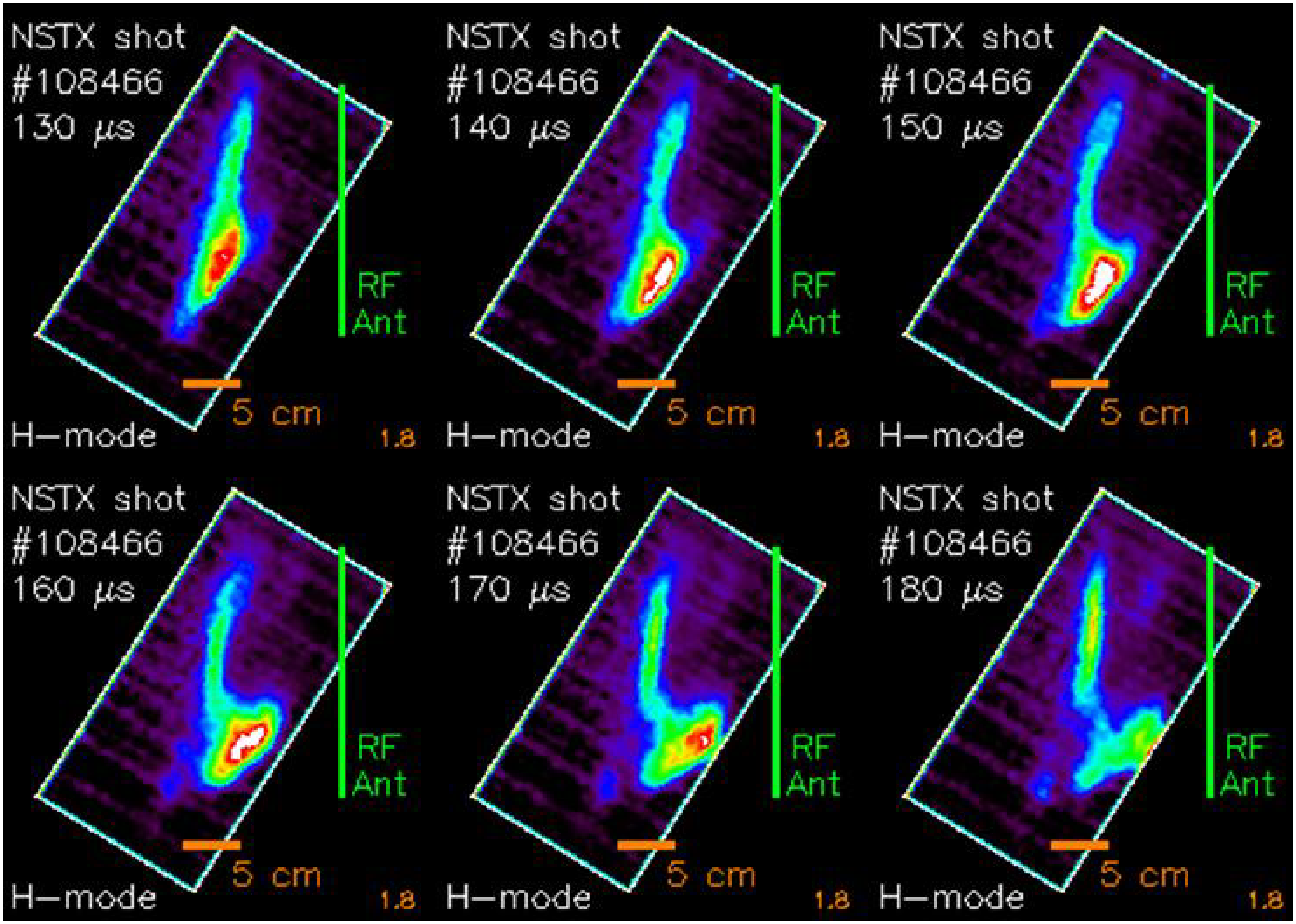

"Target Plane" Defined by Manifold & Center Stack; Location Determined by Measuring Arm

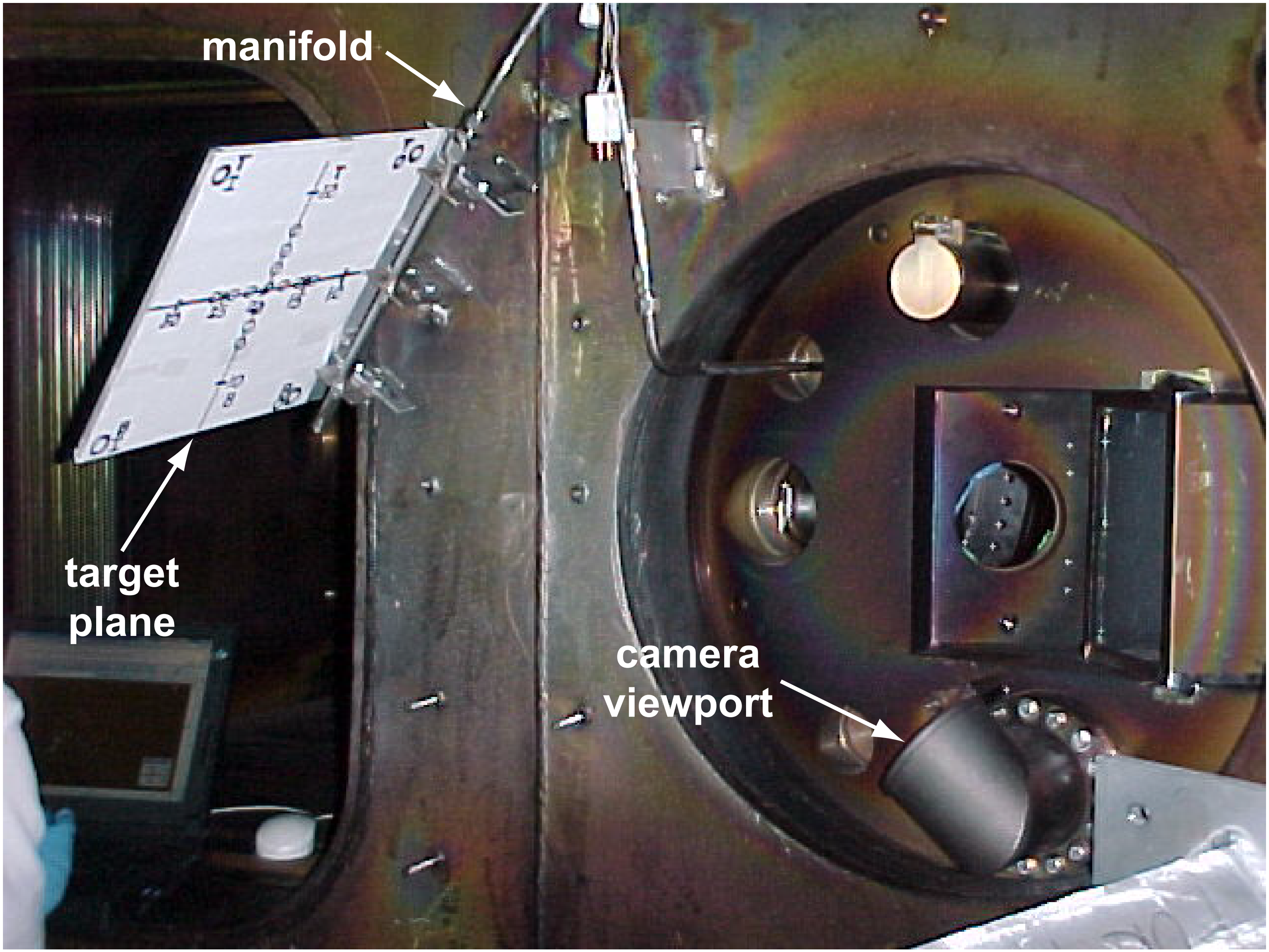

Quantify Cloud Orientation By Fitting Ellipses; Compare to Flux Surfaces Mapped to Target Plane

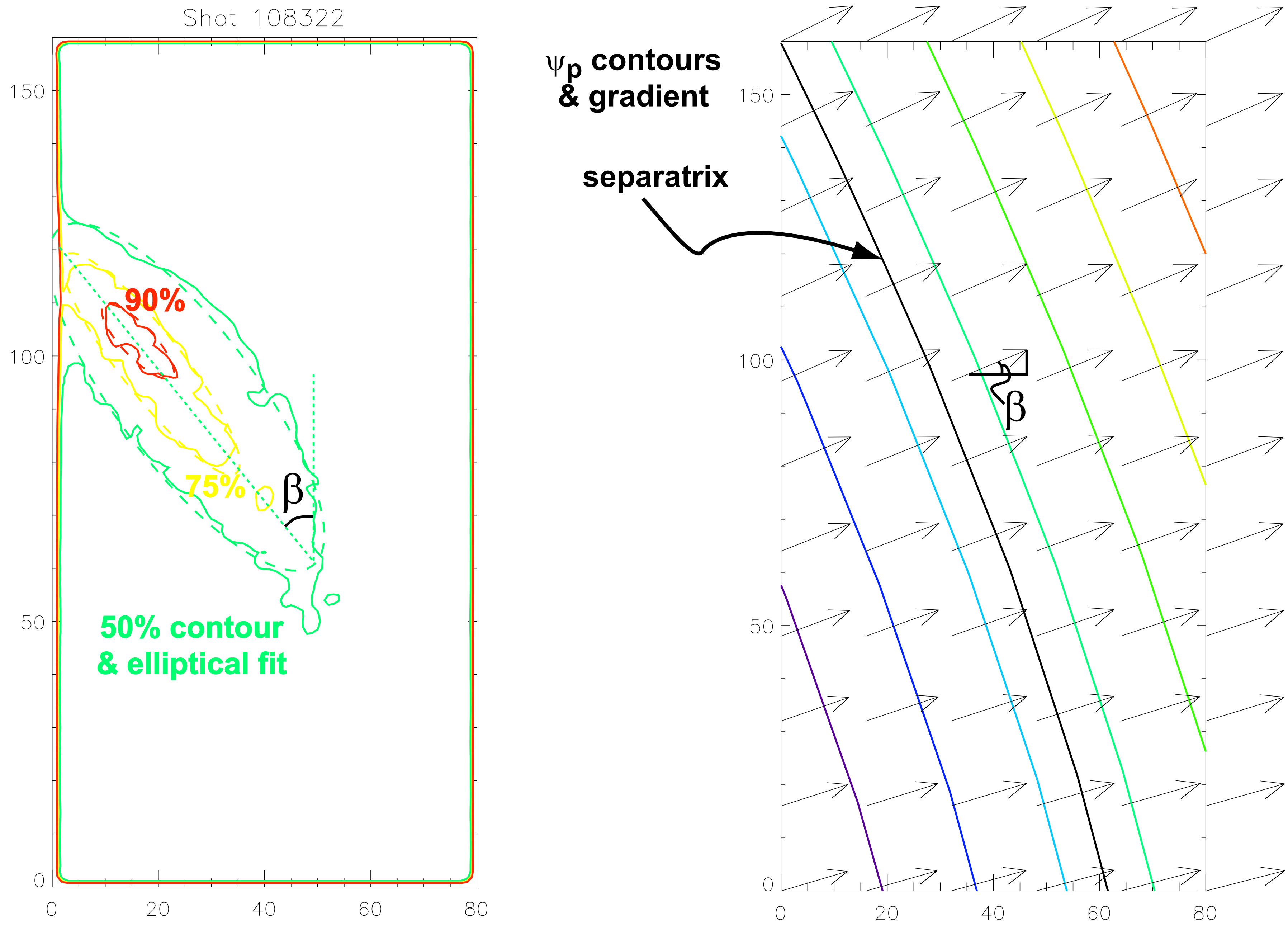

2. Construction of 3-D

DEGAS 2 Simulations

DEGAS 2 Simulation Geometry & Plasma

- Begin with outline of hardware,
- 2-D plasma mesh defined using EFIT equilibrium,
- Fill remaining volume with triangles, spatial resolution $\sim$ few mm.
- Divide into 3-D by $\phi =$ constant planes,
  - Gas source simulated in 3-D.
- Single-time $n_e(R_{\rm mid})$, $T_e(R_{\rm mid})$ from Thomson scattering,
  - Assume $n_i = n_e(\psi)$, $T_i = T_e(\psi)$ only.
- Simulations are time-independent.

Realistic, High Resolution Geometry
NSTX Shot 108321, 187 ms

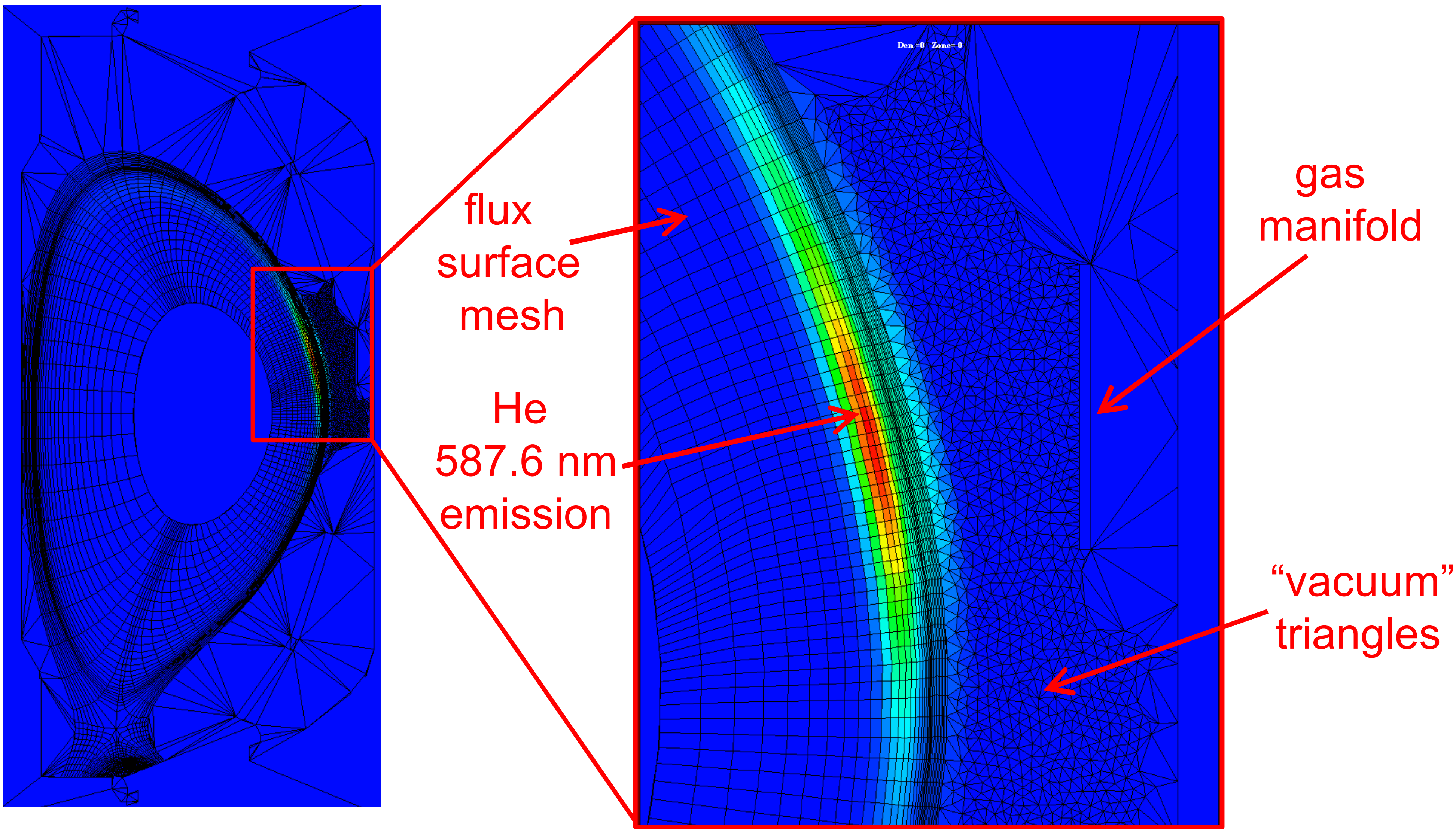

Spatial Relationships of Physical Objects Clarified by Visualization of 3-D DEGAS 2 Data

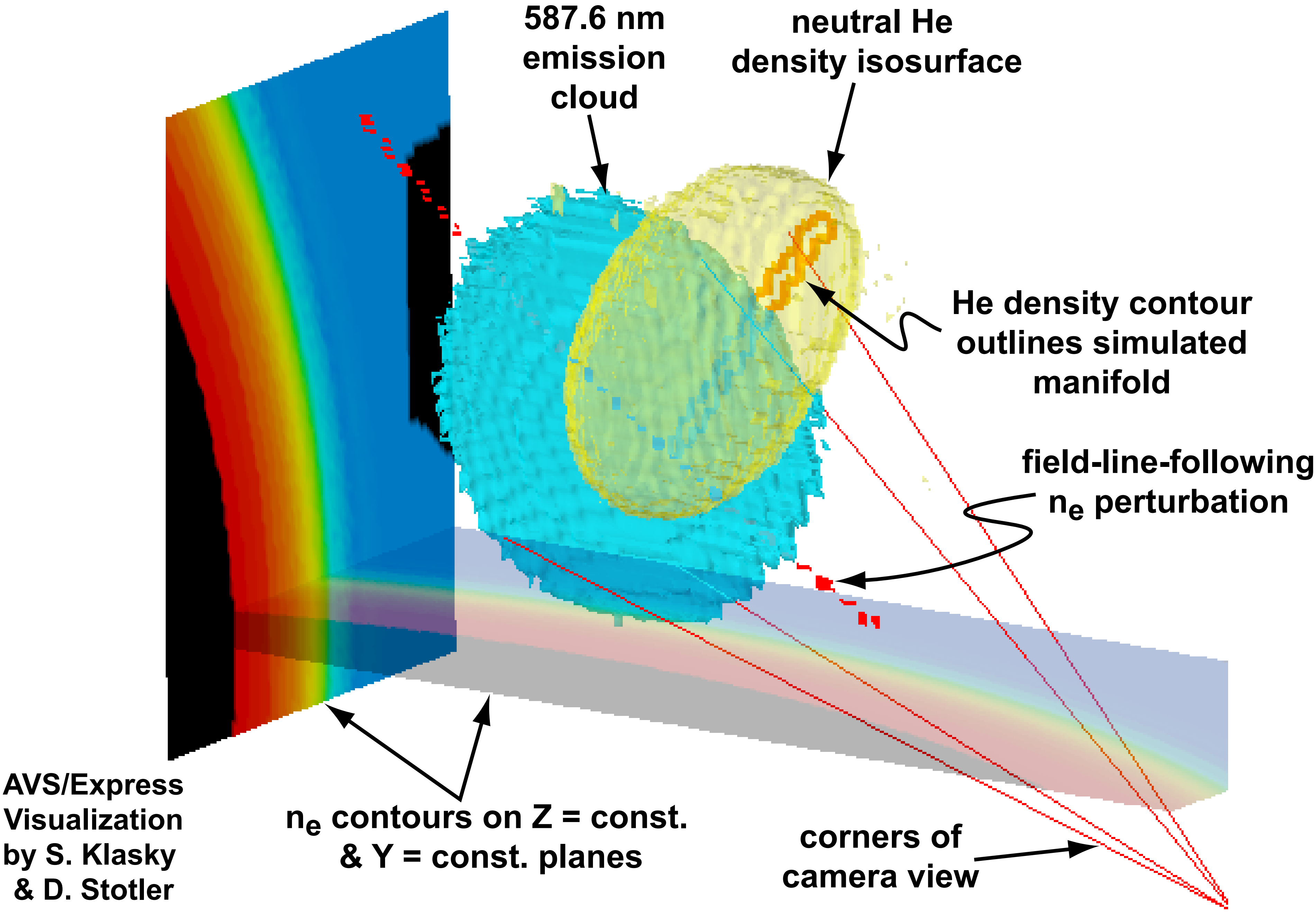

GPI Camera Emulation

- Directly compute 81×161 pixel view of camera,
- Each pixel corresponds to chord integral through problem,
- Chords start at viewport,
- Second point is measured 3-D location of intersection with “target plane”.
- Replicate 0.4 cm camera resolution with chords having halfwidth 0.16° at target plane.
- Full resolution images computed during post-processing with MPI.

3. Benchmark Code Against Experiment

Compare 3-D DEGAS 2 Camera Images With Experiment

- 3-D plasma used in DEGAS 2 *does not* correspond to a particular GPI frame $\Rightarrow$ compare with "averaged" frame,
  - Use median in time to reduce effect of blobs.
- Experimental & simulated contours angled 15°,
  - Simulated emission follows flux / plasma contours,
  - Deviation between cloud & separatrix angles noted before.
- Look for systematic variations in experimental emission cloud orientation,
  - Get flux surface angles from EFIT $\nabla\psi_p$, mapped to camera coordinates.
  - Fit ellipses to 50%, 75%, and 90% emission regions.

Observed & Simulated Cloud Orientations Differ

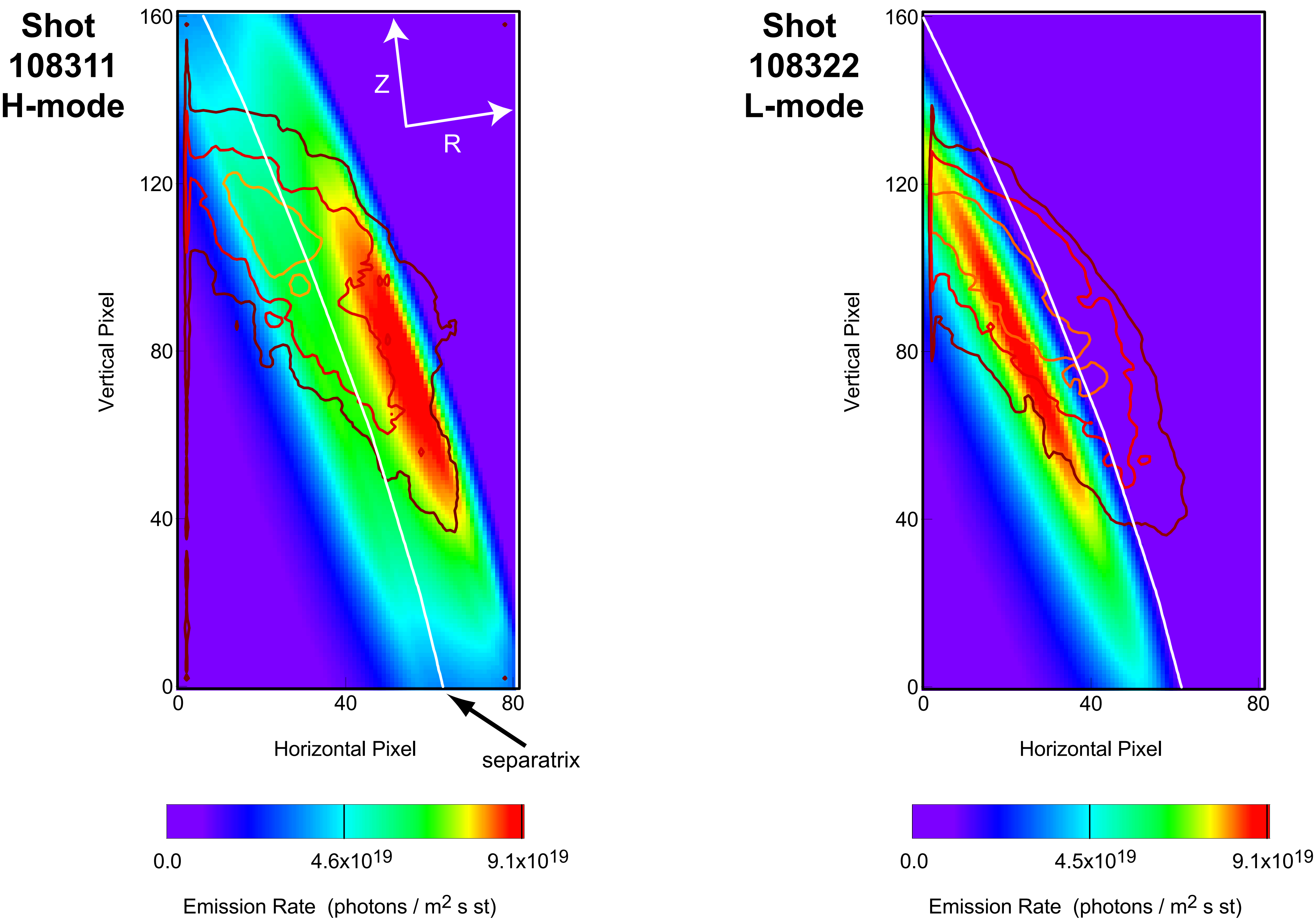

Flux Surface Angles Steady During '02 Campaign, But Emission Angles Vary

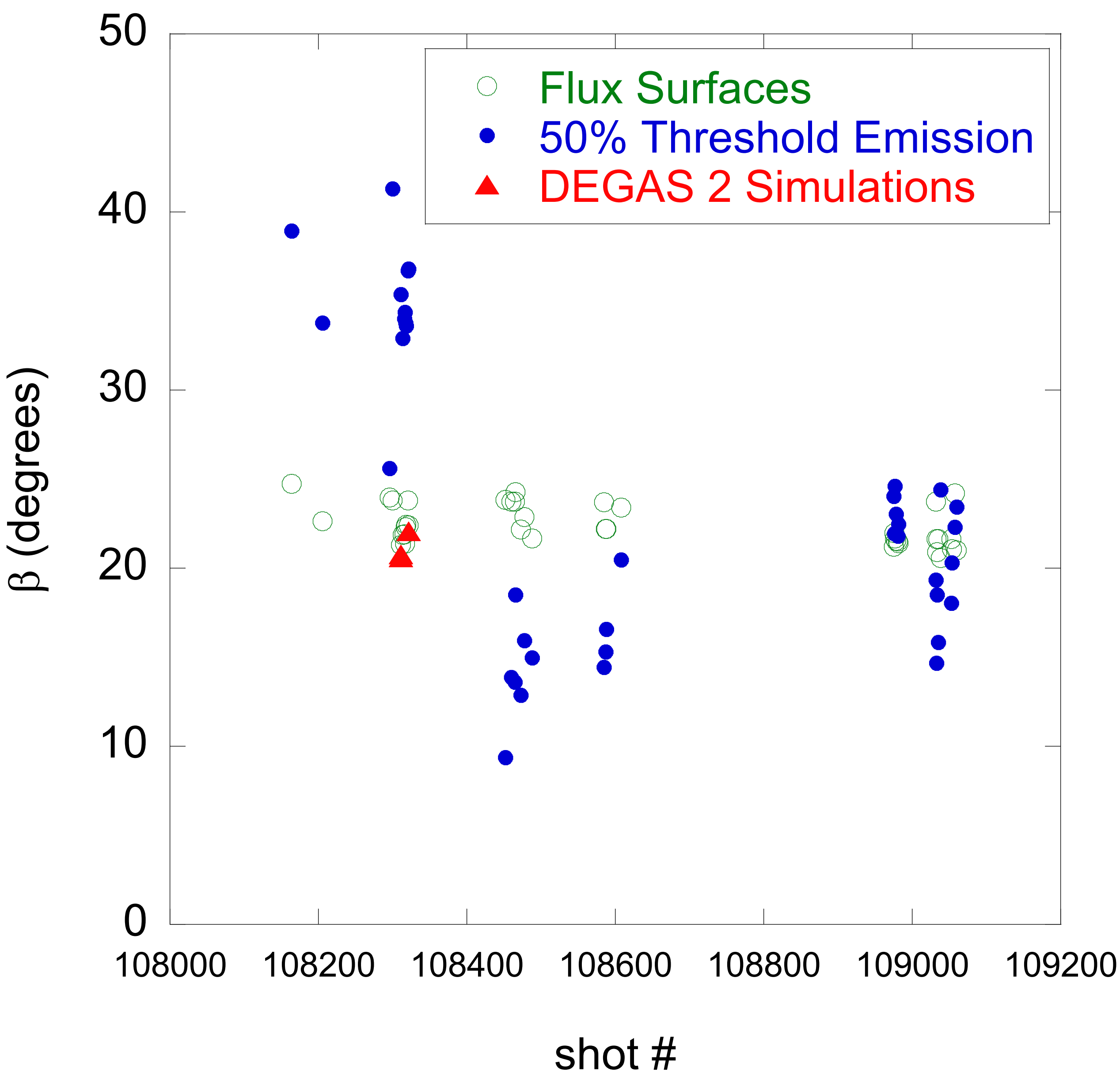

Variation of Emission Cloud Orientation Not Understood

- Systematic changes in angles after run breaks,
  - Optics were removed & replaced each time,
  - $\Rightarrow$ Discrepancy with DEGAS 2 could be due to misalignment of optical fixture or bumping of mirror.
- Calibration was done after last campaign
  $\Rightarrow$ probably why last group lines up best with flux surfaces.
- There may be yet other explanations!
- Should do DEGAS 2 simulation of shot from last group.

4. Estimate Diagnostic Resolution

Background Information

- Previous radial resolution estimate 2 ± 1 cm based on toroidal cloud width & degree of camera / field alignment,
  - Effect of latter on poloidal resolution: 0.5 – 2 cm.
- For shots used here I_p & B_T match values used in design of GPI $\Rightarrow$ can't examine misalignment,
- Check toroidal width with slices along camera view,
  1. FWHM = 25 cm for 108322,
  2. 20 cm for 108311,
  3. Observed: 24 cm.

Estimate Resolution with Tracer Perturbation

- Double n_e everywhere along field line passing through a chosen cell.
  - Estimate effect of cloud width & field line curvature.
- Relatively long emission perturbation path in camera-aligned slice
  $\Rightarrow$ field line-camera alignment is indeed good,
- $\triangle$(emission) image shows shape of field line as seen by camera, as well as shadowing effect,
  - Radial & poloidal half-widths are same as size of initial cell!
  - $\Rightarrow$ Toroidal extent of cloud *does not* significantly degrade radial resolution (at least here).

Camera-Aligned Slice Through 3-D Data Shows Emission Due to Perturbation

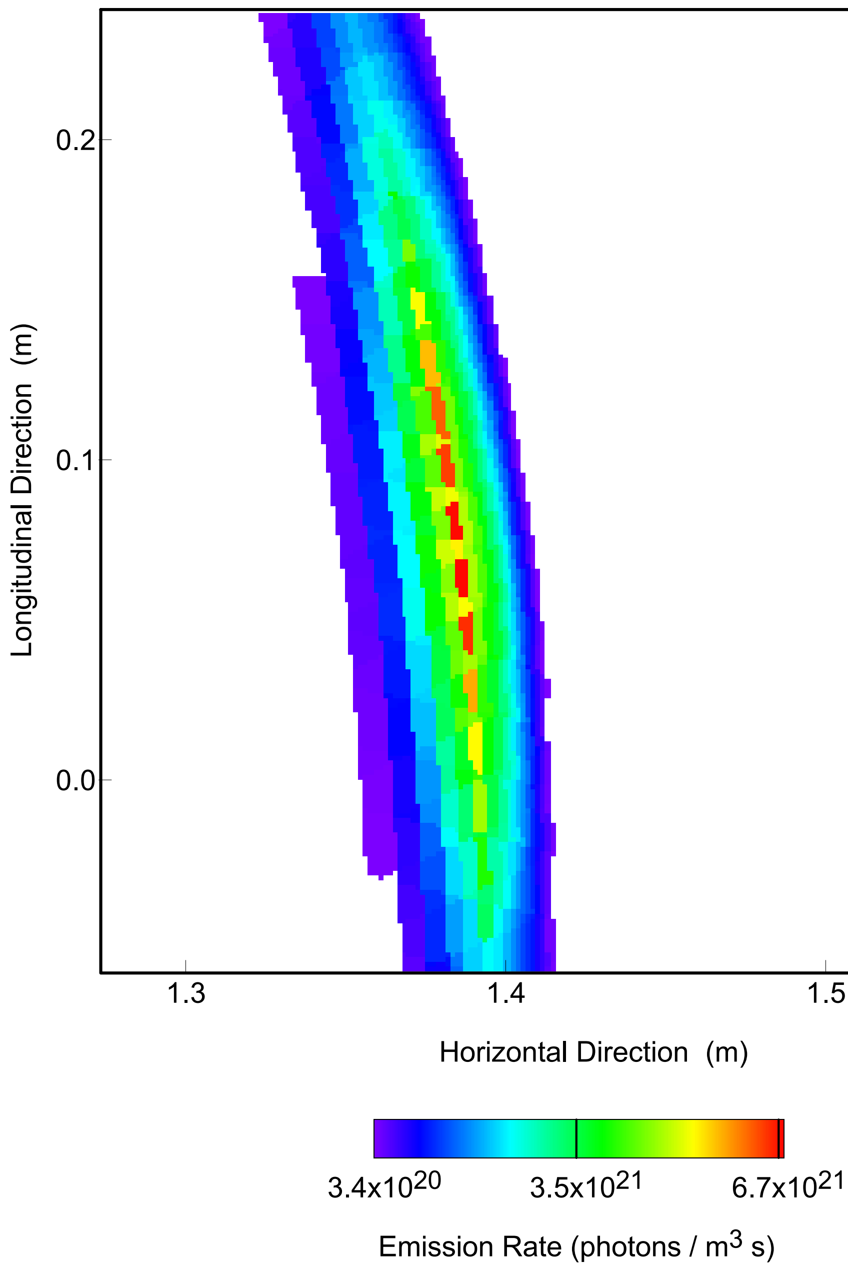

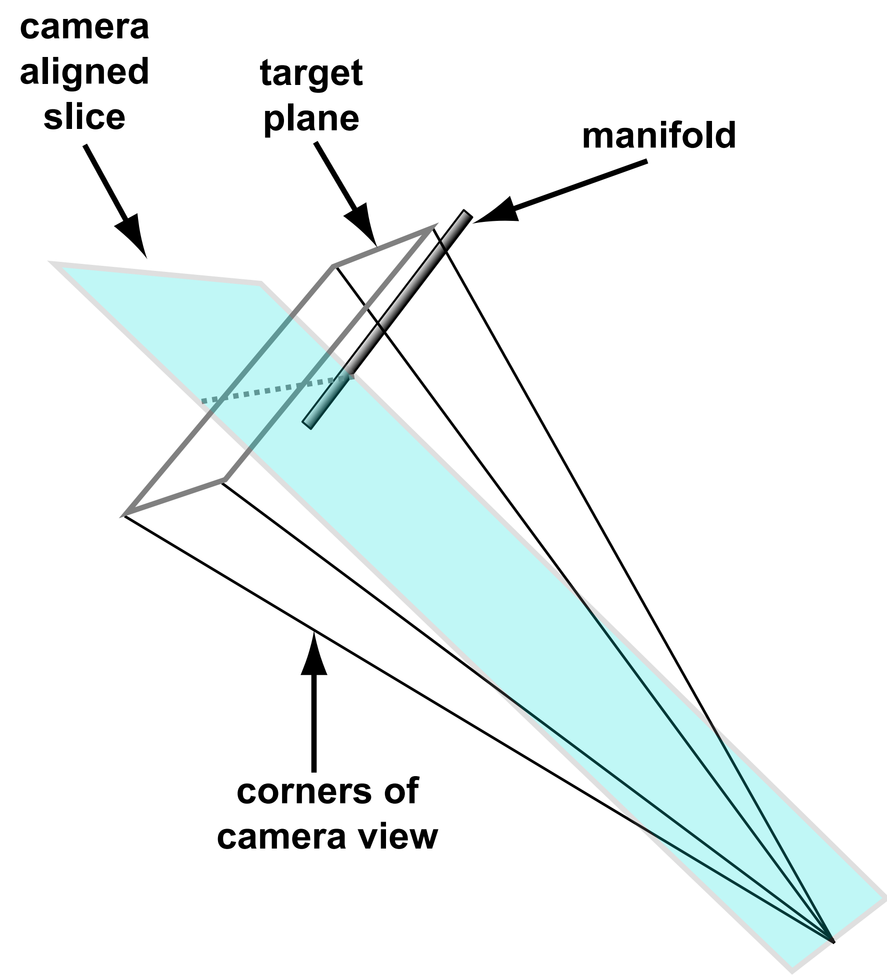

Perturbed - Unperturbed Camera Image Highlights Effect of n_e Perturbation

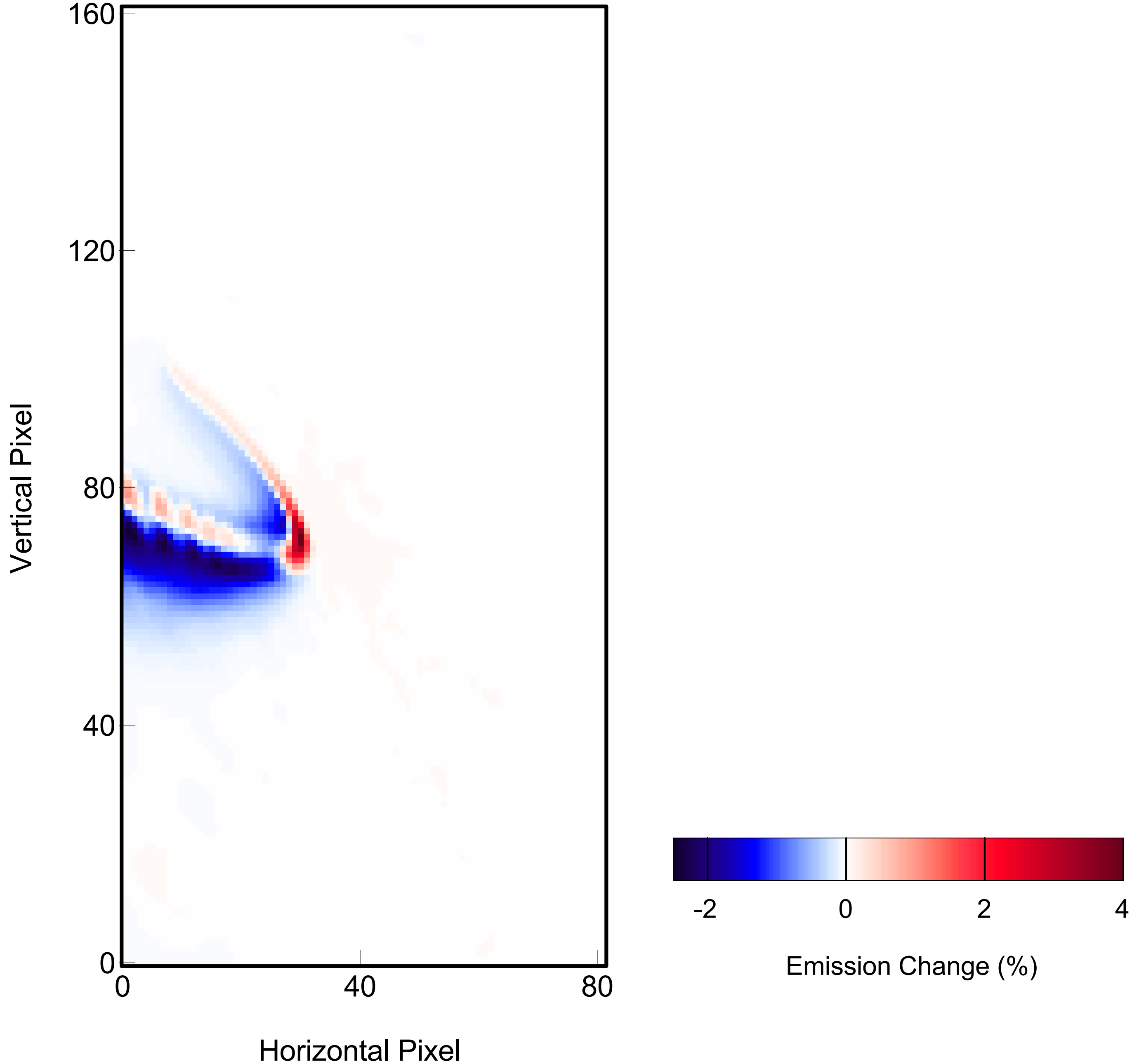

5. Use Neutral Density to Infer

2-D Plasma Profiles from GPI Images

See also poster LP1.070,

“Theory and Experimental Analysis

of Blobs in the NSTX Boundary Plasma”,

Myra et al.

GPI Data + DEGAS 2 Neutral Density $\Rightarrow$ 2-D n_e, T_e

- Use to test theories of blob motion.
  - $n_e, T_e \longrightarrow$ potential, Φ,
  - $\Rightarrow \vec{E} \times \vec{B}$ & motion of blobs.

- GPI gives $I = n_0 F(n_e, T_e)$,
  - DEGAS 2 $\Rightarrow n_0$,
  - $F(n_e, T_e)$ known,
  - $\Rightarrow$ can invert if we know $n_e(T_e)$.

Need to Map 3-D DEGAS 2 Neutral Density to 2-D Camera Coordinates

- Camera signal for pixel i:

$$I(i) = \int \frac{dl}{4\pi} F(\vec{x}) n_0(\vec{x}).$$

- $\vec{x}$ and image coordinates i connected by target plane, $\vec{x}_i$,
  - Inversion will yield $n_e(\vec{x}_i)$ and $T_e(\vec{x}_i)$.

- Camera aligned with $\vec{B}$ & blobs constant on $\vec{B} \Rightarrow F(\vec{x}) \sim F(\vec{x}_i) =$ constant,

$$I(i) \simeq F(\vec{x}_i) \int \frac{dl}{4\pi} n_0(\vec{x}).$$

- Suggests using

$$n_{0,\text{eff}} \equiv \int \frac{dl}{4\pi} n_0(\vec{x}) \simeq I(i)/F(\vec{x}_i).$$

Effective Neutral Density in Camera Coordinates

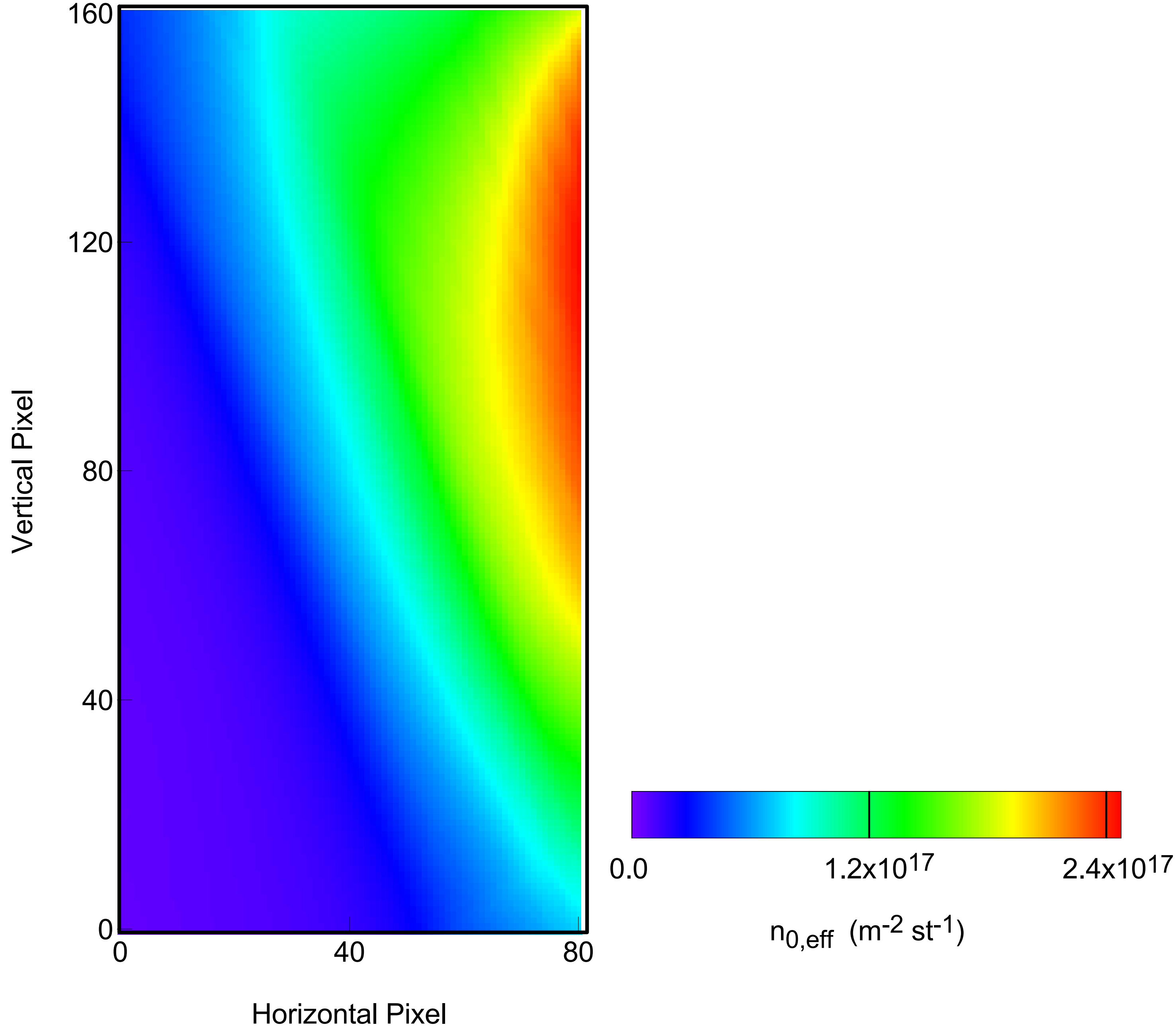

Practical Applications of Effective Neutral Density

- Above approach is approximate, off by factor of a few,
  - Have slightly different, more accurate approach.
- But, existing simulations differ too much from observations,
  - DEGAS 2 $n_{0,\text{eff}}$ must be shifted & rotated to line up emission clouds,
  - In this case, the two approaches work equally well.
  - See poster by Myra et al., LP1.070 for example applications.

SUMMARY

- 3-D DEGAS 2 simulations of GPI reproduce experimental geometry in detail,

- Orientations differ by 15°,
  - Appears to be due to GPI optical alignment problem with shots early in 2002 campaign.

- Radial resolution not significantly degraded by toroidal extent of cloud.

- DEGAS 2 results provide basis for inferring time-dependent 2-D n_e, T_e from GPI data.

Note: This poster is available on the Web at:
`http://w3.pppl.gov/degas2/`

REFERENCES

- R. J. Maqueda et al., Rev. Sci. Instrum. **74**, 2020 (2002)
  - NSTX GPI description.
- S. J. Zweben et al., Nucl. Fusion, (2003) (to be published)
  - Detailed analysis of NSTX GPI results.
- D. P. Stotler and C. F. F. Karney, Contrib. Plasma Phys. **34**, 392 (1994)
  - Basic DEGAS 2 description.
- D. P. Stotler et al., J. Nucl. Mater. **313–316**, 1066 (2003)
  - DEGAS 2 simulations of C-Mod GPI.
- S. I. Krasheninnikov, Phys. Lett. A **283**, 368 (2001)
  - Basic theory of blobs.

- D. A. D'Ippolito et al., Phys. Plasmas **9**, 222 (2002)
  - Theory of blob motion.
- D. A. D'Ippolito et al., Contrib. Plasma Phys., (2003) (PET9)
  - Ditto.
- M. Goto, J. Quant. Spectrosc. Radiat. Transfer **76**, 331 (2003)
  - He collisional-radiative model.
- P. S. Krstic and D. R. Schultz, J. Phys. B **32**, 3485 (1999)
  - Neutral-ion elastic scattering data.
- S. J. Zweben, et al., Phys. Plasmas **9**, 1981 (2002)
  - Discussion of C-Mod GPI, including DEGAS 2 results.